scientific reports

Check for updates

OPEN

Study on properties of straw fiber steel slag foam concrete

Yang Liu[1,2], Shijie Fan[3], Qing Li[3], Hongbao Liang[1]✉, Xiaoyu Wang[1] & Jiaxi Xu[3]

The objective of this scholarly endeavor is to engineer an innovative, eco-friendly construction material, specifically straw fiber steel slag foam concrete (SFSSFC), with the dual purpose of optimizing resource utilization and mitigating energy expenditure within the construction sector. Through meticulous manipulation of the constituent ratios of steel slag powder, straw fiber, and foam, a series of 15 SFSSFC specimens were fabricated. Subsequent to their preparation, a comprehensive evaluation was conducted to ascertain their fluidity, water absorption, mechanical strength, thermal conductivity, and resistance to freeze-thaw cycling. The findings revealed that an increment in foam content correlates with enhanced fluidity and water absorption characteristics of the concrete matrix. Furthermore, it was determined that a 15% steel slag powder content yielded the most favorable mechanical strength outcomes. Notably, specimens incorporating 3% straw fiber displayed the lowest thermal conductivity among the evaluated samples. In assessing durability, the F10, F15, S15, and C3.0 specimens demonstrated exceptional resilience, enduring 50 cycles of freeze-thaw exposure without incurring damage. Comparative analysis with extant literature suggests that the SFSSFC developed in this study exhibits superior thermal and mechanical properties.

Keywords Foamed concrete, Steel slag, Straw fiber, Fluidity, Water absorption, Mechanical properties, Thermal conductivity, Freeze-thaw properties

The construction sector is a pivotal yet energy-intensive industry, contributing over 30% to global energy consumption[1]. This figure underscores the urgency for sustainable practices, especially considering the high energy and carbon emissions associated with traditional cement production, which conflict with the carbon neutrality goals of many developing nations[2]. In this context, the quest for energy-efficient building materials has become a research imperative. Among emerging alternatives, foamed concrete stands out for its superior thermal and acoustic insulation properties, economic feasibility, and reduced environmental impact[3]. Its sustainability is further enhanced by the substitution of cement and sand with waste materials, addressing carbon dioxide (CO_2) emissions, natural resource depletion, and waste management in the construction sector[4].

Steel slag, a by-product of steel manufacturing, accounts for approximately 15% of crude steel output[5]. In 2020, China's steel slag production was projected to reach 160 million tons, yet less than 30% was effectively utilized[6,7]. Untreated steel slag not only consumes valuable land resources but also poses a significant environmental risk through heavy metal ion contamination, leading to ecological damage[8,9]. Studies have shown that the incorporation of steel slag into foamed concrete can increase water absorption and alter bending strength in a non-monotonic manner[10]. The potential economic and environmental benefits of using steel slag as a substitute for cement or fine aggregate have been highlighted[11]. Research has also focused on determining the optimal replacement ratio of steel slag for cement in foamed concrete to maintain compressive strength[12]. Additionally, the impact of steel slag powder on the compressive performance of foamed concrete has been explored, revealing its ability to promote the formation of calcium silicate hydrate (C-S-H) gel, densify the microstructure, reduce pore size, and enhance compressive strength[13].

Natural fibers, once a staple in construction, have experienced a resurgence due to the industry's demand for low-energy consumption materials[14]. Despite the rise of industrialization, urbanization, and commercialization, natural fibers such as corn, rice, bamboo, flax, and coir are now being re-evaluated for their potential in construction, particularly in resource-rich nations like China, Brazil, and India[15–21]. China's corn production is anticipated to exceed 1.5 billion tons by 2022[22].

The incorporation of natural fibres was found to substantially enhance the tensile, flexural strengths and fracture toughness of cement matrices[23–26]. Owing to their dispersion effect, these fibres can effectively control crack formation and propagation, thereby inducing a transition from the inherent brittle failure mode of cement matrices to a more desirable ductile one[27–29].Beyond this, the addition of natural fibres leads to an

[1]School of Mechanical Science and Engineering, Northeast Petroleum University, Daqing 163318, China. [2]The College of Architecture and Civil Engineering, Qiqihar University, Qiqihar 161006, China. [3]School of Architecture and Civil Engineering, Northeast Petroleum University, Daqing 163318, China. ✉email: lhb19661009@163.com

improvement in the impact resistance and an augmentation in the overall toughness of the material1. Research has confirmed that natural fibres can reduce the shrinkage of cement matrices, especially in dry environments. This modification plays a crucial role in mitigating the risk of shrinkage-induced cracks, thus enhancing the material's durability[30]. Natural fibres can also effectively suppress crack formation and propagation through their dispersion within the cement matrix. They achieve this by bridging cracks and slowing down the rate of crack propagation[28]. As a result, the crack-resistance of the material is significantly improved. Despite these benefits, the incorporation of natural fibres may slightly increase the water absorption of cement matrices (usually by approximately 8%), which could potentially lead to debonding issues at the fibre - matrix interface[30,31]. However, by optimizing the fibre dosage and employing appropriate treatment methods, the adverse effects can be effectively mitigated. The utilization of natural fibres not only elevates the performance of cement matrices but also brings about environmental advantages. As renewable resources, natural fibres can diminish the reliance on conventional synthetic fibres, consequently reducing the carbon footprint[31]. The combination of natural fibres with materials such as alccofine can further optimize the mechanical properties of cement matrices. Studies have demonstrated that when bamboo fibres (BF) and coconut shell fibres (CF) are used in conjunction with alccofine, the mechanical properties of concrete are remarkably enhanced[32].

The utilization of corn stalk fiber in construction materials represents a significant advancement in sustainable resource management. This agricultural byproduct, often regarded as waste, can be transformed into a valuable resource for the construction industry, thereby reducing waste accumulation and promoting resource efficiency[33]. This circular approach helps to diminish reliance on natural resources and eases environmental burdens[34]. When compared to traditional construction materials, the production process of corn stalk fiber is less energy-intensive and requires minimal chemical treatment, resulting in reduced carbon emissions[35]. Additionally, substituting petroleum-based materials with corn stalk fiber contributes to a further reduction in carbon footprint[34]. Research has demonstrated that the incorporation of corn stalk fiber into building materials can significantly enhance the flexural strength, tensile strength, and durability of these materials[36]. Furthermore, materials derived from corn stover exhibit remarkable fire resistance, chemical durability, and thermal insulation properties[37]. The low cost and wide availability of corn stalk fiber make their application in construction materials economically viable1. Large-scale application can potentially lower the overall cost of construction materials while providing an additional source of income for farmers1. The application of corn stalk fiber aligns with the principles of sustainable development by addressing agricultural waste disposal issues and offering an eco-friendly alternative in the construction sector[36]. The promotion of this material can drive the development of green building practices and foster a harmonious balance between ecological conservation and economic benefits[38].

Despite existing studies on foam concrete incorporating steel slag and corn stalk fiber, significant knowledge gaps persist. The understanding of the optimal replacement ratios of steel slag in foam concrete, particularly when combined with corn stalk fiber, remains limited. The complex interactions between steel slag, corn stalk fiber, and the foam concrete matrix are not yet fully elucidated. Additionally, the long-term performance, durability, and environmental impact of these composite materials require further investigation.Specifically, while individual studies have explored the effects of steel slag and corn stalk fiber on foam concrete properties, few have systematically examined their combined influence. The potential synergistic effects of these components on the material's mechanical strength, thermal insulation, and acoustic properties are not well understood. Furthermore, the impact of varying fiber types, sizes, and treatments on the overall performance of steel slag foam concrete remains an area ripe for exploration. The influence of environmental factors, such as humidity and temperature fluctuations, on the durability of these composites over time is also not adequately addressed in existing literature.

This research aims to bridge these knowledge gaps by systematically investigating the properties of steel slag foam concrete reinforced with corn stalk fiber. By optimizing the replacement ratios and understanding the interactions between components, we can develop a high-performance, sustainable construction material with broad applicability. The successful integration of steel slag and corn stalk fiber into foam concrete will not only enhance the material's mechanical and physical properties but also contribute to the circular economy by utilizing industrial byproducts and agricultural waste.From an environmental perspective, this research will help reduce the carbon footprint of construction materials by decreasing reliance on traditional energy-intensive components like cement and sand. The utilization of steel slag and corn stalk fiber will also alleviate waste management challenges and minimize the depletion of natural resources. Economically, the development of a cost-effective and sustainable building material can benefit the construction industry by reducing material costs and providing new revenue streams for waste generators.

Overall, this research holds significant promise for advancing the sustainability of the construction sector, supporting global carbon neutrality efforts, and promoting the efficient use of resources through innovative material solutions.

Test programme

Materials

In this investigation, specimens of foam concrete were meticulously fabricated through the utilization of a domestic Portland cement of the P.O42.5 grade, complemented by steel slag powder (SSP), fly ash, corn straw fiber (CSF), and silica ash. The mechanical and physical properties of CSF were presented in Table 1, thereby offering a comprehensive overview of its characteristics pertinent to this study. Additionally, the chemical composition of the materials employed is detailed in Table 2, which is crucial for understanding their reactivity and potential interactions within the composite material. The foaming agent employed in this research is a protein-based blowing agent, the physical properties of which are outlined in Table 3. This choice of foaming agent is significant as it influences the cellular structure and, consequently, the insulative and mechanical properties of the foam

Fiber type	Length (mm)	Breadth (mm)	Density (g/cm^3)	Tensile strength (MPa)	Elastic modulus (GPa)
Filament	10	0.5-1	13	65	15

Table 1. Mechanical and physical characteristics of the CSF.

Raw materials	CaO	MgO	Al_2O_3	SO_3	Fe_2O_3	SiO_2	LOI
P.O 42.5 OPC	63.58	2.56	7.00	1.92	2.96	16.07	3.76
Steel slag	37.29	4.55	14.22	2.84	1.49	35.01	4.6
Fly ash	9.47	2.74	25.1	0.61	3.59	52.98	5.51
Silica fume	0.31	0.39	0.16	0.21	0.03	96.42	2.48

Table 2. The chemical composition of the materials utilized in this paper.

Physical attributes	Density (kg/l)	PH VALUE	Chloride content (Cl)	Alkali content	Freezing point
Synthetic liquid air-entraining	1.05 ± 0.02	4.5 ± 1	< 0.1%	< 5%	− 5 °C

Table 3. The properties of the foam agent used in this paper.

Sample component	OPC	Foam	Steelslag	Cornstalk	Flyash	Silicafume	Water − reducingagent	Water
F0	496	0	200	8	80	24	7	220
F10	496	80	200	8	80	24	7	220
F15	496	120	200	8	80	24	7	220
F20	496	160	200	8	80	24	7	220
F25	496	200	200	8	80	24	7	220
F30	496	240	200	8	80	24	7	220
S0	696	160	0	8	80	24	7	220
S10	616	160	80	8	80	24	7	220
S15	576	160	120	8	80	24	7	220
S20	536	160	160	8	80	24	7	220
S25	496	160	200	8	80	24	7	220
S30	456	160	240	8	80	24	7	220
C0.0	496	160	200	0	80	24	7	220
C1.0	496	160	200	8	80	24	7	220
C1.5	496	160	200	12	80	24	7	220
C2.0	496	160	200	16	80	24	7	220
C2.5	496	160	200	20	80	24	7	220
C3.0	496	160	200	24	80	24	7	220

Table 4. The mixing ratio of all SFSSFC samples (kg/m^3).

concrete. The specific surface area of the Portland cement, a key parameter affecting hydration and strength development, is quantified at 325 m^2/kg, with a specific gravity of 3.05, indicating its density and potential impact on the concrete's rheological properties.

Sample Preparation

Initially, the foaming agent is combined with water at a ratio of 1:50 and agitated in a mixing vessel for 25 min to generate foam. Subsequently, varying quantities of solid constituents are intimately blended with water according to the mixing proportions detailed in Table 4, yielding a slurry after 2 min of mixing in a mixing vessel. Subsequently, foam concrete of varying foam qualities was fabricated. The foam was carefully prepared and then transferred into a beaker for integration with the pre-mixed slurry. This initial mixture was manually agitated for a duration of 2 min to ensure thorough blending. Thereafter, the mixture underwent mechanical agitation at a moderate rotational velocity of 120 revolutions per minute (r/min) for an additional 3 min to achieve a homogeneous blend. This process results in the formation of foam concrete specimens with varying dimensions: 100 mm×100 mm×100 mm, 40 mm×40 mm×160 mm, 300 mm×300 mm×30 mm, and 100 mm × 100 mm × 400 mm. Subsequently, the freshly mixed foam concrete specimens were demoulded and subjected to a curing process within a stringent environmental chamber, where the temperature was meticulously controlled

at 20 ± 2 °C, and the relative humidity was maintained at no less than 95%. This curing regimen was executed for discrete periods of 7, 14, and 28 days, prior to the commencement of mechanical and durability assessments. In the purview of this investigation, a comprehensive set of 15 unique specimen groups were meticulously crafted to evaluate the effects of varying foam, steel slag, and straw contents on the performance metrics of the foam concrete. These groups were systematically designed to provide a nuanced understanding of the interplay between composition and material performance[39]. The precise mixing proportions for these specimen groups are articulated in Table 4, which serves as a critical reference for the methodology and subsequent data analysis.

Test procedure

The rheological properties of the foamed concrete were evaluated in strict accordance with the protocols detailed in GB/T2419-2005[40]. Concurrently, the determination of dry density and water absorption was executed following the methodologies prescribed in JG/T266-2011[41]. For these specific tests, specimens underwent a curing process prior to being subjected to a controlled drying regime at 60 °C for a period of 24 h, after which their masses were meticulously recorded[42]. Figure 1[43] presents a comprehensive flowchart of the water absorption test, which serves as a critical indicator of the material's long-term durability. The assessment of mechanical strength, thermal conductivity, and freeze-thaw resistance was conducted in compliance with the Chinese standards GB/T50081-2019[44], JGJ/T341-2014[45], and GB/T50082-2009[46], respectively (Fig. 2).

Compressive and tensile strengths were ascertained for each set of triplicate specimens, each measuring 100 mm × 100 mm × 100 mm, using an electro-hydraulic servo universal testing machine (WAW-1000 W). The flexural strength of three prismatic specimens, each with dimensions of 40 mm×40 mm×160 mm, was evaluated using an electric cement folding testing machine (DKZ-5000), employing a loading rate of 50 N/s[47]. Thermal conductivity was analyzed for specimens measuring 300 mm×300 mm×30 mm utilizing a thermal constants analyzer (TPS2200), while the freeze-thaw resistance of quintuplicate specimens, each measuring 100 mm×100 mm×400 mm, was assessed using a concrete rapid freeze-thaw testing machine (HC-HDK9), with a series of cycles ranging from 10 to 50.

Results and discussion

Fluidity

As depicted in Fig. 3a, the flowability of foam concrete exhibits a positive correlation with the proportion of foam content. When the foam content is elevated to 30%, the flowability reaches its peak at 241 mm, a finding that is in accordance with prior research. This enhancement in flowability can be attributed to the lubricating action of the foam. The foam reduces the frictional forces between the constituent particles and facilitates greater water incorporation within the mixture, both of which contribute to an improvement in the overall flowability of the foam concrete.

Figure 3b illustrates that the flowability of foam concrete demonstrates an upward trend as the steel slag powder content is increased from 10 to 30%, with corresponding flowability values rising from 151 mm to 183 mm. The addition of steel slag powder plays an effective role in suppressing bubble coalescence. This leads to a more uniform distribution of auxiliary pores within the foam concrete matrix, thereby enhancing the flowability. This phenomenon can be ascribed to the specific particle shape and size distribution of steel slag powder, which is conducive to optimizing the pore structure of the foam concrete and improving its flowability.

From Fig. 3c, it can be observed that the flowability of foam concrete experiences a slight decline as the rice straw fiber content is increased. Specifically, when the fiber content is raised from 1 to 3%, the flowability decreases from 173 mm to 160 mm, marking a reduction of 7.0%. The maximum flowability of 173 mm is achieved at a rice straw mass fraction of 1%. The incorporation of rice straw fibers tends to increase the friction between the materials, which in turn results in a slight diminution of flowability. This is predominantly because the fibrous structure of rice straw fibers has the effect of increasing the viscosity of the concrete mixture and impeding its flow. Nevertheless, the decrease in flowability is not substantial and can be mitigated through the implementation of appropriate mix design strategies and fiber surface treatments.

Water absorption

Figure 4a illustrates a linear correlation between the water absorption rate and foam content in foam concrete. Initially, water absorption decreases with increasing foam content, reaching a minimum of 10.5% at 10% foam content (sample F10). However, further increases in foam content lead to a rise in water absorption, with sample F30 (30% foam content) exhibiting the highest rate of 23.3%. This trend is attributed to the dual role of foam in

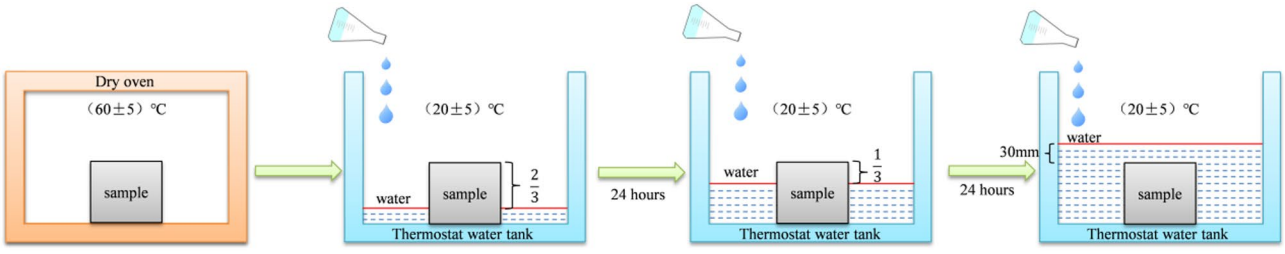

Fig. 1. Concrete water absorption test diagram.

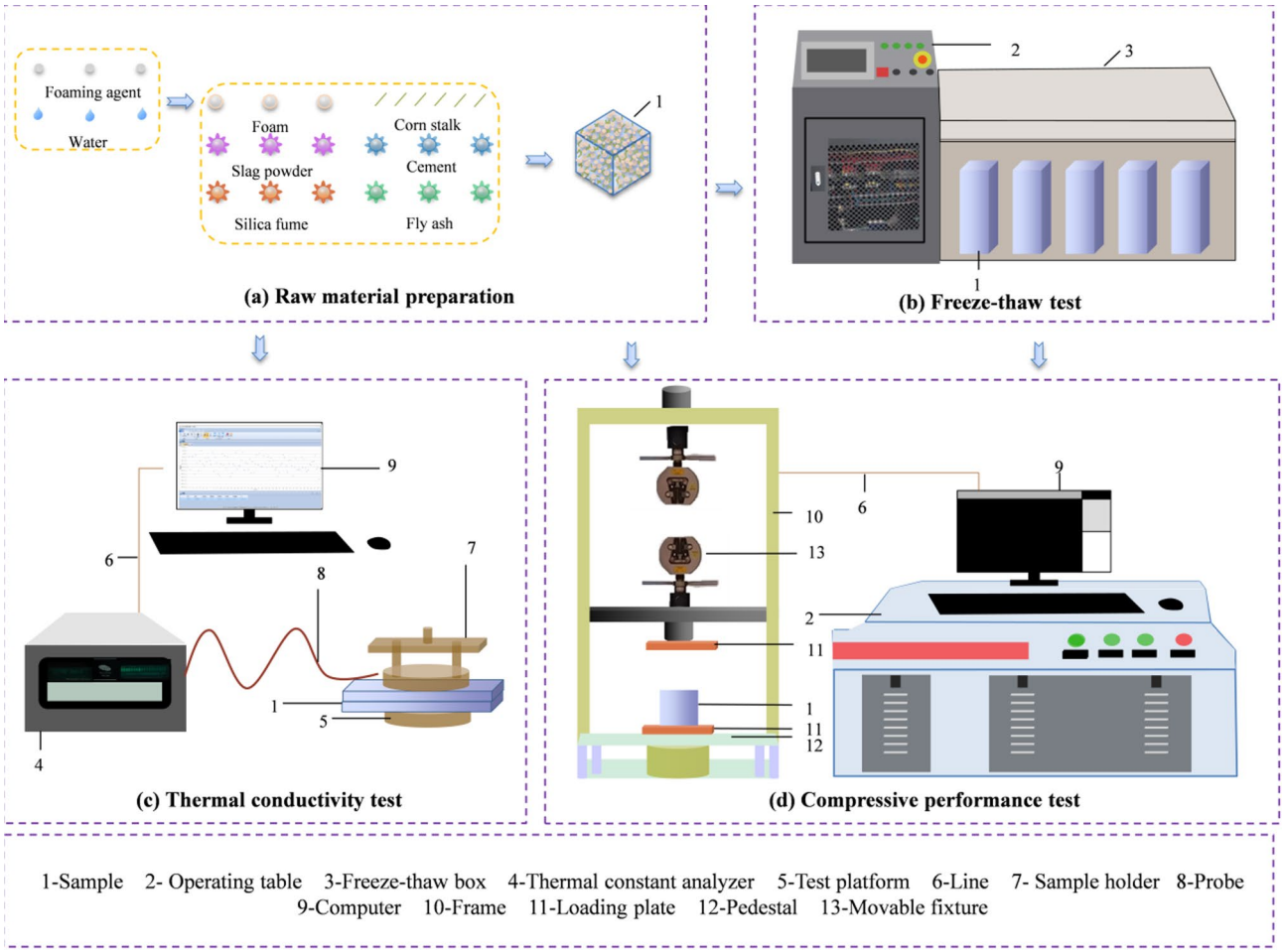

Fig. 2. Fabrication process of concrete specimens and associated testing apparatus.

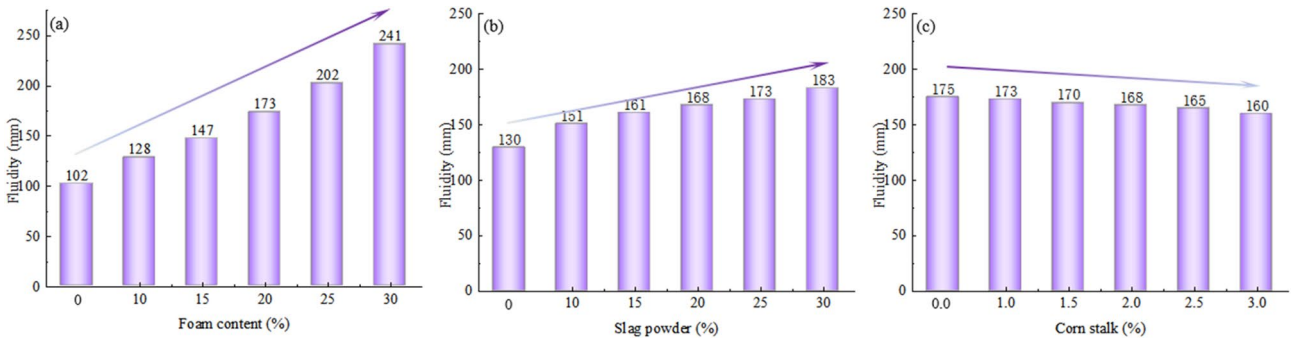

Fig. 3. (**a**) Foam (**b**)slag powder (**c**) corn stalk on the fluidity of the foamed concrete specimens.

pore structure development. At moderate levels, foam aids in forming a stable pore network that limits water penetration. Excessive foam, however, disrupts this balance by introducing overly porous regions and uneven foam distribution, which can create interconnected pore pathways that facilitate water ingress.

As shown in Fig. 4b, the relationship between water absorption and steel slag powder content in foam concrete exhibits a U-shaped trend. When the steel slag powder content increases from 10 to 15%, water absorption decreases from 15.5 to 14.4%. However, further increasing the steel slag powder content to 30% results in an increase in water absorption to 17%. This behavior can be attributed to the pozzolanic activity of steel slag powder. Within the optimal range of 10–15%, the steel slag powder actively participates in secondary hydration reactions, which refine the pore structure, reduce pore size, and enhance the concrete's water resistance. The formation of additional hydration products such as calcium silicate hydrate (C-S-H) contributes to a denser microstructure. Beyond 15%, the excessive addition of steel slag powder may lead to an overabundance of

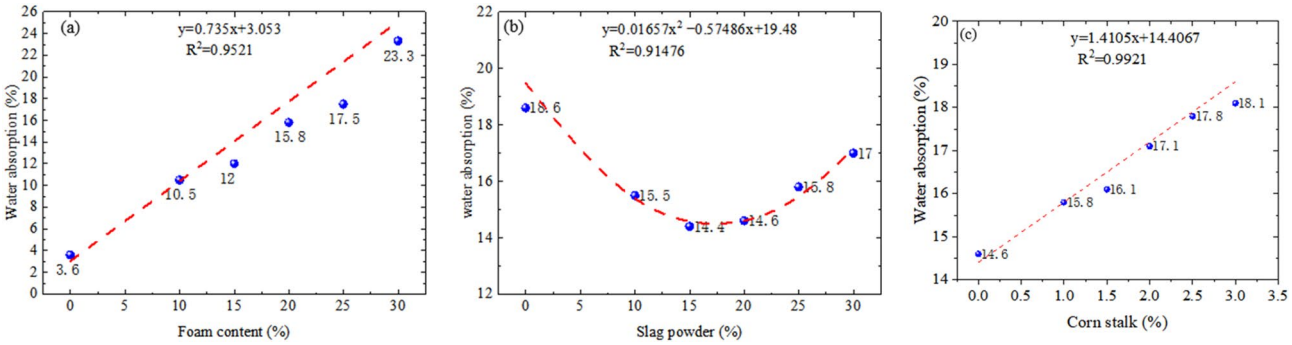

Fig. 4. (**a**) Foam (**b**) Slag powder (**c**) Corn stalk on the water absorption of the foamed concrete specimens.

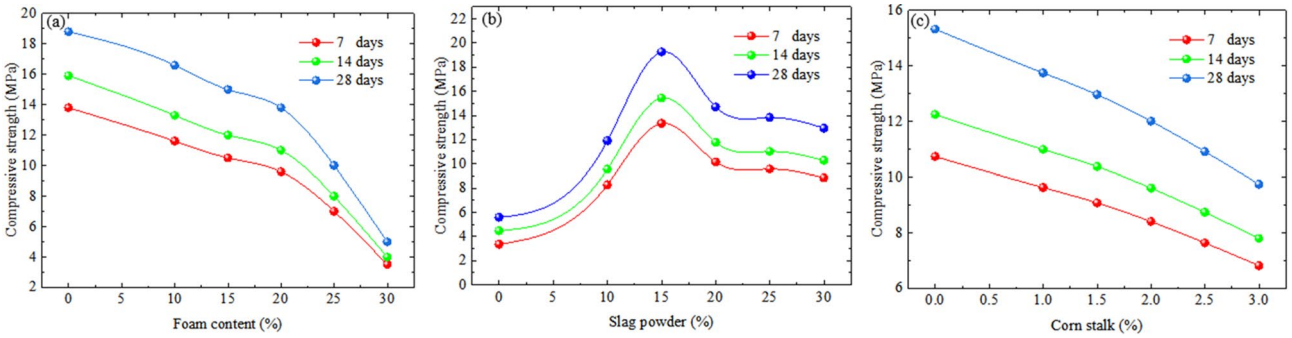

Fig. 5. (**a**) Foam (**b**) Slag powder (**c**) Corn stalk on SFSSFC specimen compressive strength.

reactive materials, which can disrupt the balance of the cementitious system. This may result in a less uniform distribution of hydration products, potentially creating weaker points within the matrix. Additionally, the increased quantity of steel slag powder could dilute the cement paste, reducing its binding efficiency and leading to a less compact concrete structure. The combination of these factors—microstructural inhomogeneity and reduced paste density—likely contributes to the observed increase in water absorption at higher steel slag powder contents.

Figure 4c reveals a direct linear relationship between water absorption and rice straw fiber content in foam concrete. This suggests that increasing rice straw fiber content can effectively reduce water absorption. The fibrous structure of rice straw fibers allows them to bridge pores within the concrete, blocking water penetration pathways and reducing pore connectivity. Furthermore, the hygroscopic nature of rice straw fibers enables them to absorb a portion of the water, further lowering the concrete's water absorption rate. These characteristics make rice straw fibers a valuable addition for enhancing the water resistance of foam concrete.

Mechanical strength

This section provides a detailed exposition on the effects of diverse constituents on the mechanical strength of the foamed concrete developed in this study, assessed at specific curing intervals of 7, 14, and 28 days. Figure 5 delineates the variation in compressive strength with incremental increases in foam content, steel slag powder content, and straw fiber content. From Fig. 5a, it is observed that as the foam content escalates from 10 to 30%, there is a corresponding decline in compressive strength. Specifically, the 7-day strength reduces from approximately 11.6–3.5 MPa, marking a 70% decrease. The 14-day strength decreases from about 13.3–4.0 MPa, a 70% reduction. The 28-day strength also diminishes from about 16.6 MPa to 5.0 MPa, representing a 58% decline. The present study reveals the significant impact of the foam mass fraction on the compressive strength of foamed concrete. An elevation in the proportion of foam within the concrete matrix results in a reduced interfacial bond and an increased volumetric ratio of pores, which logically culminates in a reduction of compressive strength[52]. The decrease in compressive strength from the 7-day to the 28-day mark is markedly more pronounced as the foam mass fraction escalates from 20 to 30%, with a decrease exceeding 60%. Consequently, it is inferred that the optimal foam mass fraction in the foamed concrete examined herein should not exceed 20% to maintain adequate compressive strength.

Figure 5b illustrates the effect of steel slag powder content on the compressive strength of foamed concrete. The results indicate that increasing the steel slag powder content from 10 to 15% significantly enhances compressive strength at 7, 14, and 28 days, with improvements exceeding 60%. However, further increases in steel slag powder content from 15 to 20% and from 20 to 30% result in a marked decrease in compressive strength by over 20% each time, leading to a gradual decline to below 8%.

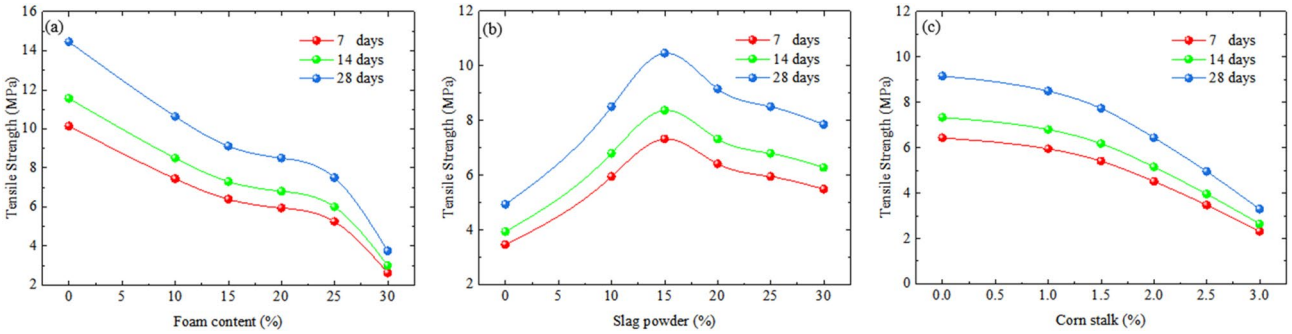

Fig. 6. (**a**) Foam (**b**) Slag powder (**c**) Corn stalk on the flexural strength of the foamed concrete specimens.

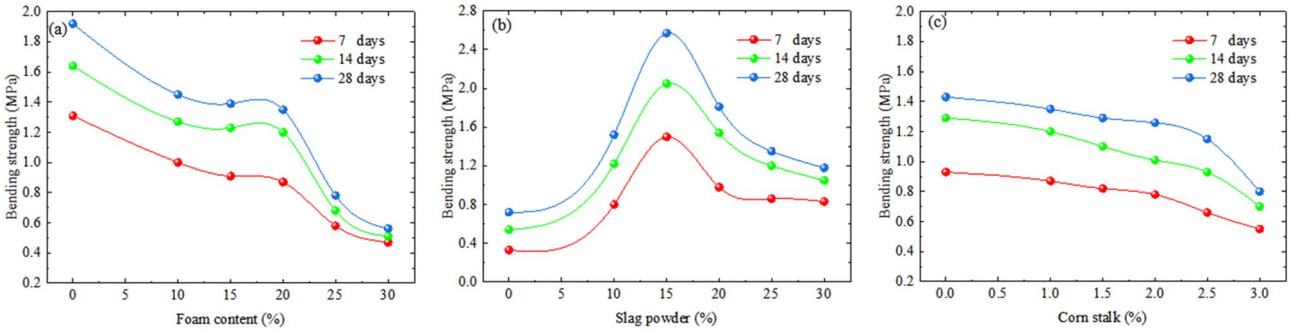

Fig. 7. (**a**) Foam (**b**) Slag powder (**c**) Corn stalk on the bending strength of the foamed concrete specimens.

The initial increase in compressive strength at 10–15% steel slag powder content can be attributed to the pozzolanic reaction of the slag. In this range, the steel slag powder dissolves effectively in the alkaline environment of OPC, releasing silicate and aluminate ions. These ions react with Ca(OH)2 to form additional C-S-H gel, which refines the pore structure and enhances the strength of the cementitious matrix. The formation of a denser and more uniform microstructure contributes to the improved compressive strength observed in this range.

Conversely, at higher steel slag powder contents (above 15%), the system may become oversaturated with reactive slag components. This can lead to a reduction in the available Ca(OH)2, which is necessary for the formation of C-S-H gel. The excess slag may also introduce microstructural inhomogeneities, such as poorly hydrated regions or increased porosity, which can act as weak points within the matrix. Additionally, the increased slag content may dilute the cement paste, reducing its binding efficiency and leading to a less compact and weaker concrete structure. These factors collectively contribute to the observed decrease in compressive strength at higher steel slag powder contents.

Figure 5c delineates the variation in compressive strength associated with the incremental increase in the mass fraction of straw fiber within the foamed concrete matrix. A marked escalation in straw fiber content from 1 to 3% is correlated with a corresponding decline in compressive strength. Specifically, the 7-day compressive strength experiences a reduction from approximately 9.6–6.8 MPa, representing a 29% decrease. The 14-day strength diminishes from about 11.0–7.5 MPa, a 32% decrease; the 28-day strength also declines from about 13.8–9.5 MPa, a 31% reduction. The experimental outcomes demonstrate that, despite the low mass fraction of straw, its impact on the compressive strength of foamed concrete remains notably significant, approximately 30%, with a more uniform trend in the decline of compressive strength.

Figure 6 illustrates the variation in tensile strength with incremental increases in foam content, steel slag powder content, and straw fiber content. As depicted in Fig. 6a, a linear decrease in tensile strength is observed as the foam content escalates from 10 to 30%, with a reduction exceeding 60% at the 7, 14, and 28-day marks.

Figure 6b presents a detailed analysis of the influence of steel slag powder content on the tensile strength of foamed concrete. The data indicates that an increment in steel slag powder from 10 to 15% yields a significant enhancement in tensile strength, exceeding 20% at all three-time points of 7, 14, and 28 days. Conversely, a further increase from 15 to 30% results in a notable decrease in tensile strength, approximately 25%.

Figure 6c illustrates the variation in tensile strength with the incremental rise in straw fiber content. An elevation in the straw mass fraction from 1 to 3% corresponds to a decrease in tensile strength, with a reduction surpassing 60% at the 7, 14, and 28-day intervals. These findings suggest that the effects of steel slag powder and straw fiber content on the tensile strength of foamed concrete are congruent with their influence on compressive strength.

Figure 7 provides a comprehensive depiction of the alterations in flexural strength with respect to incremental increases in the content of foam, steel slag powder, and straw fiber within the foamed concrete matrix. Specifically,

Fig. 7a illustrates that an escalation in foam content from 10 to 30% is accompanied by a corresponding decline in flexural strength, with a reduction exceeding 50% at the 7, 14, and 28-day assessment points.

Furthermore, Fig. 7b elucidates the influence of varying steel slag powder content on the flexural strength of foamed concrete, offering insights into how this particular constituent affects the material's performance under bending loads. The data indicates that augmenting the steel slag powder content from 10 to 15% results in a significant enhancement in flexural strength by over 65% at all three-time points; conversely, a further increment from 15 to 30% leads to a marked decrease in flexural strength by more than 45%.

Figure 7c illustrates the alteration in flexural strength associated with the incremental rise in straw fiber content. An elevation in the straw mass fraction from 1 to 3% is accompanied by a decrease in flexural strength, with a reduction surpassing 35% at the 7, 14, and 28-day intervals.

The mechanical strength of foamed concrete is intrinsically linked to its dry apparent density, as documented in the literature[39,53]. Figure 8 presents the correlation function between the compressive strength ascertained in this investigation and the corresponding apparent dry density reported in other scholarly works. The compressive strength results obtained in this study, as presented in Table 5, exhibit both consistencies with and deviations from existing literature. These results align with the performance criteria stipulated in the Chinese standard JG/T 266–2011[42]. Across the dry density range of 600–800 kg/m^3, our findings of 2.4–7.3 MPa align with previous studies. Similarly, at 800–1000 kg/m^3, our compressive strength values of 1.3–7.4 MPa fall within documented ranges. However, discrepancies emerge at higher densities: for the 1000–1400 kg/m^3 range, our results of 5.0-19.3 MPa are slightly lower than the literature's 6.7–21.4 MPa; and at 1400–1700 kg/m^3, our compressive strength values of 13.8–16.6 MPa show a narrower distribution compared to the literature's 12.9–27.7 MPa. At the highest density range of 1700–2100 kg/m^3, direct comparison with our results is not feasible based on the available literature.

These differences can be attributed to the unique composition of the foam concrete in our study. The specific combination of foam content, steel slag, and corn straw fibers influences the porosity and pore structure of the concrete. Higher foam content increases porosity but may compromise the optimal pore distribution, thereby reducing strength. Furthermore, the integration of steel slag and corn straw fibers affects the mechanical

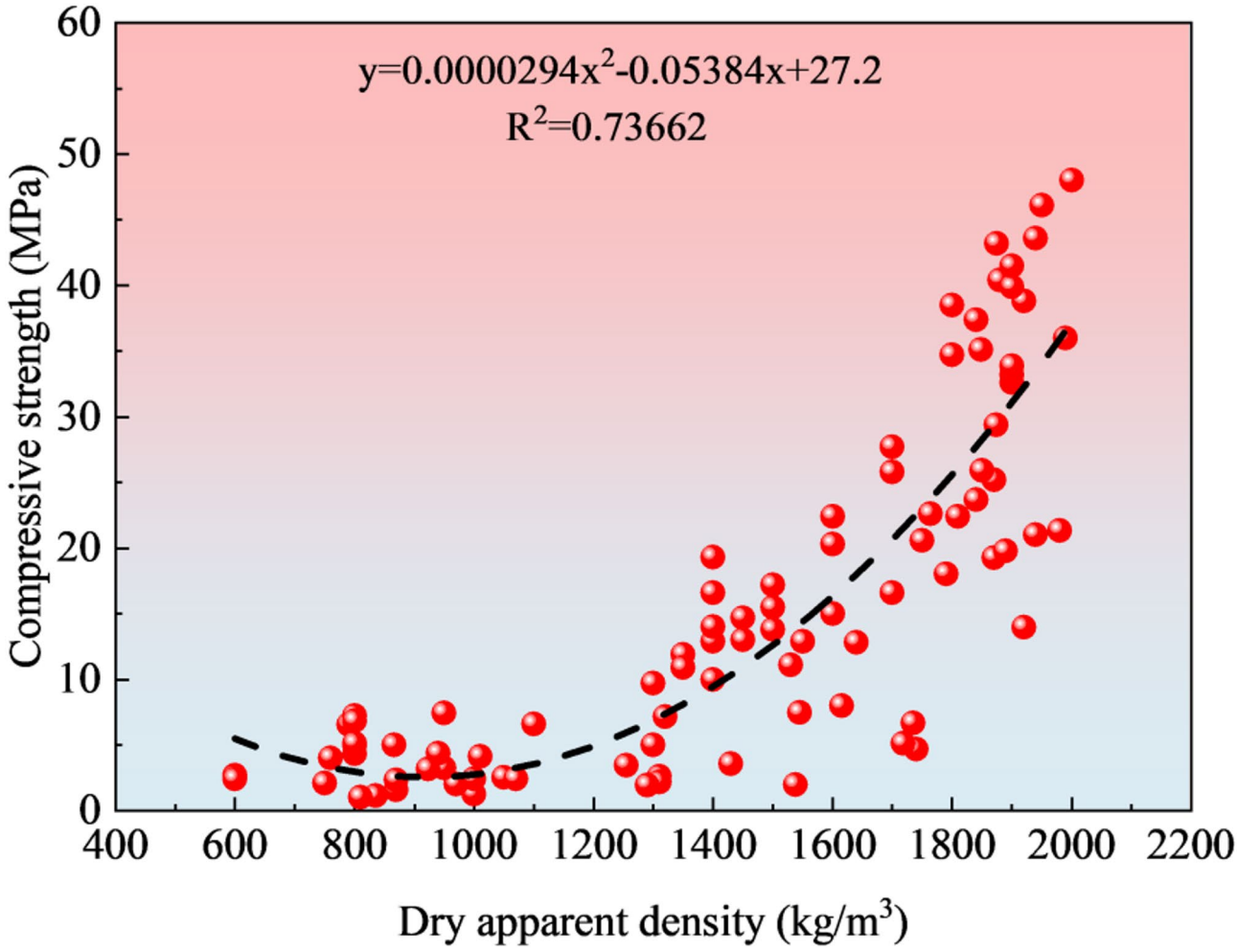

Fig. 8. Correlation between compressive strength and dry apparent density of foamed concrete specimens in this investigation.

Dry density (kg/m^3)	Compressive strength (28 days) (MPa)		References
	Other literature	This study	
600–800	2.4–7.3		55–58
800–1000	1.3–7.4		53,59–61
1000–1400	6.7–21.4	5.0-19.3	42,50
1400–1700	12.9–27.7	13.8–16.6	52,63
1700–2100	8.0–48.0		63,64

Table 5. This study presents a comparative analysis of the compressive strength results obtained from our experiments with those documented in the existing body of literature.

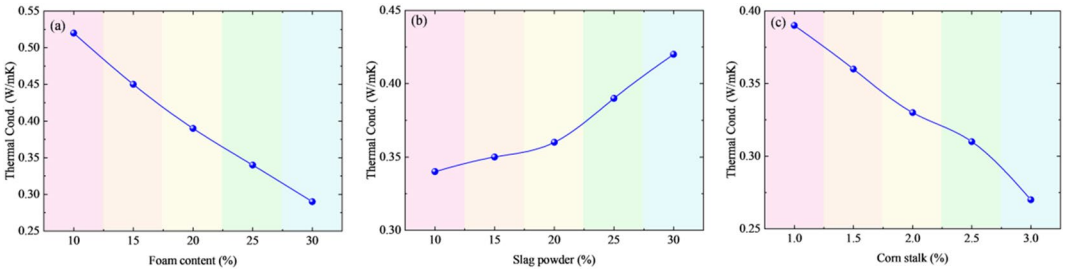

Fig. 9. (**a**) Foam (**b**) Slag powder (**c**) Corn stalk on the thermal conductivity of the foamed concrete specimens.

properties of the composite. These materials can either enhance or diminish strength depending on their processing and compatibility with the cement matrix. The distinct mix design employed in our study likely accounts for the observed variations in compressive strength compared to other research.

Thermal conductivity

Figure 9 presents the 28-day thermal conductivity outcomes for foamed concrete with varying foam, steel slag powder, and straw fiber contents. As delineated in the figure, thermal conductivity exhibits a linear decrease with an increment in foam content. The observed phenomenon is attributed to the enhanced porosity and increased gas content due to elevated foam content, which consequently diminishes thermal conductivity. Among all specimens with varying foam contents, specimen F10 exhibits the highest thermal conductivity, with a recorded value of 0.52 W/m K. For foamed concrete with 160 kg/m^3 of foam content and 8 kg/m^3 of straw fiber, the thermal conductivity increased from 0.34 to 0.42 W/m K as a result of the increased steel slag powder content. This increase is ascribed to the densification effect of steel slag powder on the concrete microstructure. Notably, the foamed concrete specimen with 160 kg/m^3 of foam content and 200 kg/m^3 of steel slag powder content exhibited the lowest thermal conductivity, with C3.0 registering a value of 0.27 W/m K. This reduction in thermal conductivity is attributed to the insulating properties of straw fibers, as corroborated by the literature[55].

A significant correlation between thermal conductivity and density is well-documented in the literature[53]. Figure 10 illustrates the regression analysis that establishes a relationship between the thermal conductivity data derived from this study and the corresponding apparent dry density, integrating our findings with data extracted from additional scholarly works. The thermal conductivity results from this study, as shown in Table 6, generally align with existing literature. At dry densities of 600–800 kg/m^3 and 800–1000 kg/m^3, our thermal conductivity values are consistent with those documented in previous studies. However, deviations occur at higher densities: for the 1000–1400 kg/m^3 range, our thermal conductivity values of 0.27–0.35 W/(m K) are slightly lower than the literature's 0.38–0.44 W/(m K); and at 1400–1700 kg/m^3, our results of 0.36–0.52 W/(m K) are lower than the literature's 0.63–0.76 W/(m K). At the highest density range of 1700–2100 kg/m^3, direct comparison with our results is not feasible based on the available literature.

The lower thermal conductivity observed in our study can be attributed to the specific combination of materials and their processing methods. The incorporation of steel slag and corn straw fibers may contribute to a more insulating pore structure or possess inherent thermal properties that reduce thermal conductivity. The unique mix design and material proportions in our study likely play a role in achieving enhanced thermal insulation properties compared to previous research. Additionally, the methods used to incorporate foam into the concrete matrix may influence the pore structure and, consequently, the thermal conductivity of the final product.

Freeze-thaw resistance

Foamed concrete, characterized by its porous structure, encapsulates a significant volume of entrained air bubbles that may coalesce to form conduits for water penetration, thereby affecting the material's freeze-thaw durability[52]. In accordance with the standard JGJ/T 341–2014[65], failure is determined when the mass loss of

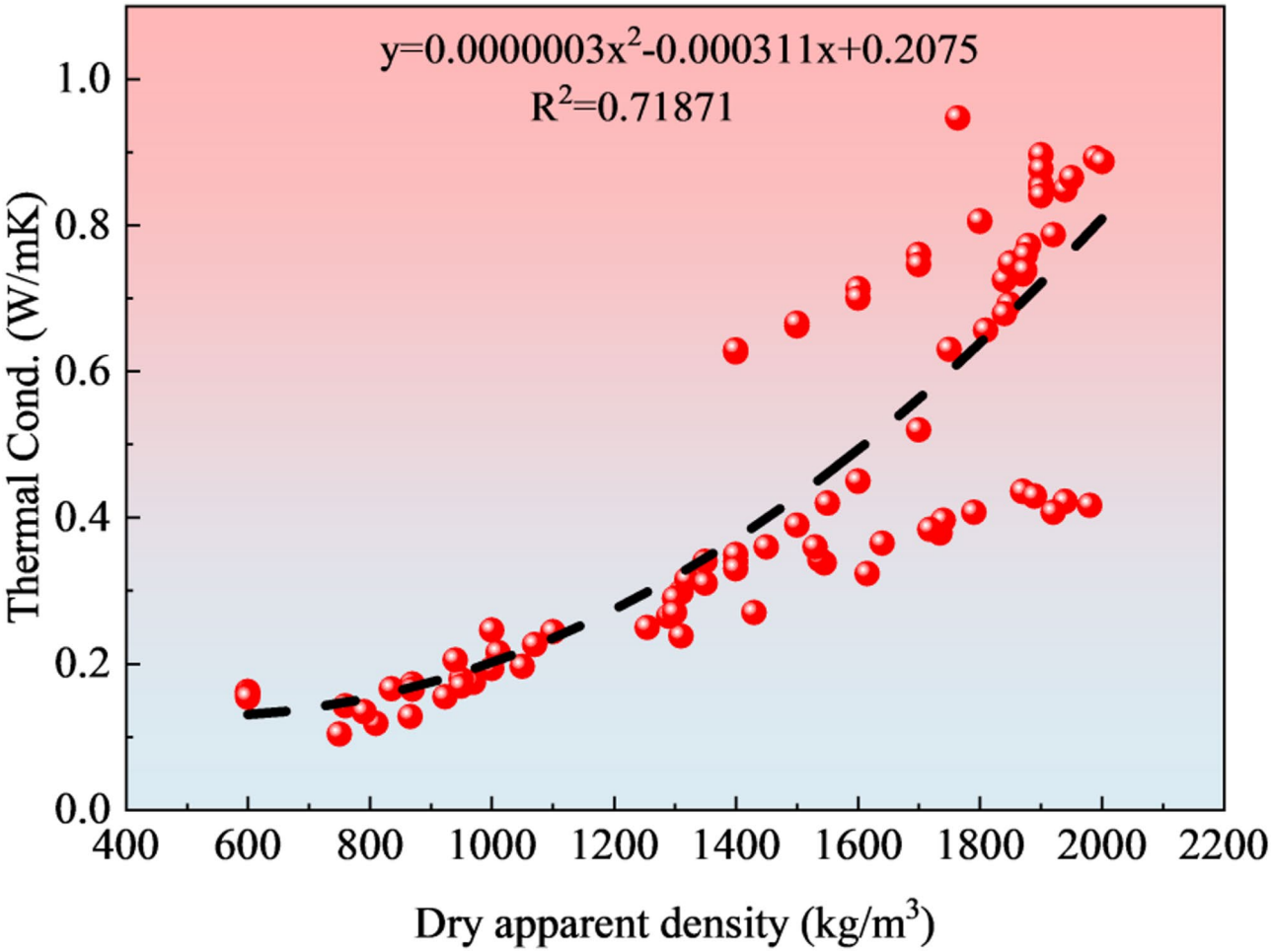

Fig. 10. The curve fitting of dry apparent density and thermal conductivity of SFSSFC.

Dry density (kg/m³)	Thermal cond.		References
	Other literature	This study	
600–800	0.15–0.16		[58]
800–1000	0.10–0.20		[53,60]
1000–1400	0.38–0.44	0.27–0.35	[55]
1400–1700	0.63–0.76	0.36–0.52	[52,63]
1700–2100	0.511-0.9		[63,64]

Table 6. The comparison between the thermal conductivity tested in this study and that reported in other literature.

foamed concrete reaches 5% or the compressive strength loss reaches 20%, with the former criterion taking precedence as the failure standard.

Figure 11 presents the mass loss and compressive strength of foamed concrete prepared with varying amounts of foaming agent following multiple freeze-thaw cycles. The results indicate that after 10 or 20 cycles, there is a marginal increase in the mass of all specimens, with a compressive strength loss ranging from 2.7 to 9.0%. This initial mass increase is posited to result from water ingress into the unsaturated specimens through interconnected pores. After 30, 40, and 50 freeze-thaw cycles, both the mass and compressive strength of the material exhibit a nearly continuous increasing trend of loss with the increase of the foaming agent dosage. Specimens F20 and F25 sustained damage when the compressive strength loss exceeded 20%, while F30 specimens were damaged when the mass loss and compressive strength loss exceeded 5% and 20%, respectively. This outcome can be attributed to the increased foam content leading to an increase in interconnected pores and water absorption, as discussed in Sect. 3.2, resulting in more water being frozen during the freeze-thaw cycles

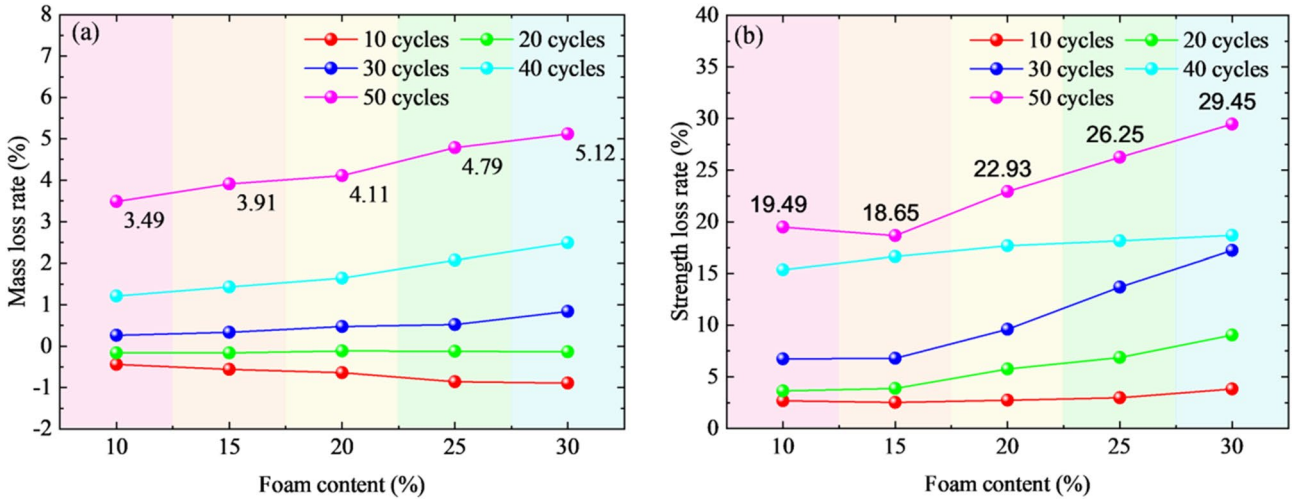

Fig. 11. (**a**) Mass loss and (**b**) compressive strength degradation of foamed concrete with varying foam content across multiple freeze-thaw cycles.

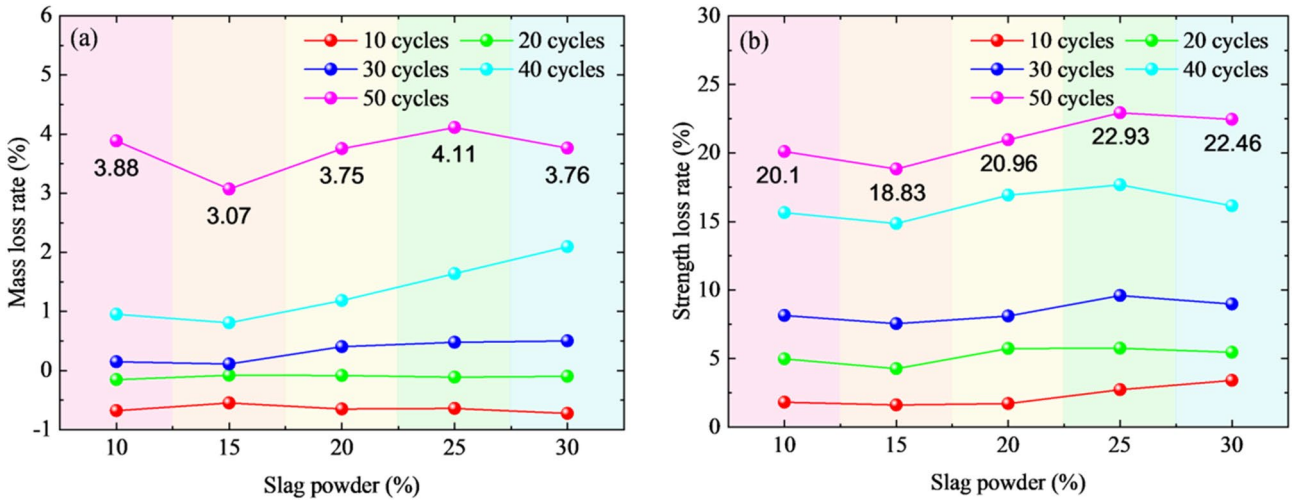

Fig. 12. (**a**) Mass loss and (**b**) compressive strength degradation of foamed concrete with varying slag powder content across multiple freeze-thaw cycles.

and a consequent increase in internal stress within the binding matrix, leading to gradual mass and compressive strength loss[39].

Figure 12 delineates the influence of steel slag powder content on the mass and compressive strength loss of foam concrete specimens. With an increase in the number of freeze-thaw cycles, there is a significant increase in mass loss and compressive strength loss of the specimens. Within 30 cycles, the difference between specimens with varying slag powder content is not significant. However, after 40 or 50 cycles, the difference becomes readily apparent, with the minimal loss of mass and mechanical strength observed in S15, which contains 15% steel slag powder in the mix ratio. This aligns with the highest flexural and compressive strength observed after 28 days of curing. Specimens S20, S25, and S30 sustained damage when the compressive strength loss exceeded 20%.

Figure 13 illustrates the influence of straw fiber content on the mass and compressive strength loss of foamed concrete specimens. An increase in straw fiber content corresponds to a decrease in the quality and compressive strength loss of foam concrete specimens, although the trend is not pronounced, likely due to the low straw fiber content. After 50 freeze-thaw cycles, no damage occurred due to mass loss in the samples; however, damage occurred when the compressive strength loss of C1.0, C1.5, C2.0, and C2.5 samples exceeded 20%. These findings underscore the significance of fiber content in enhancing the durability of foamed concrete under freeze-thaw conditions, consistent with the performance and mechanism analysis of natural fiber-reinforced foamed concrete.

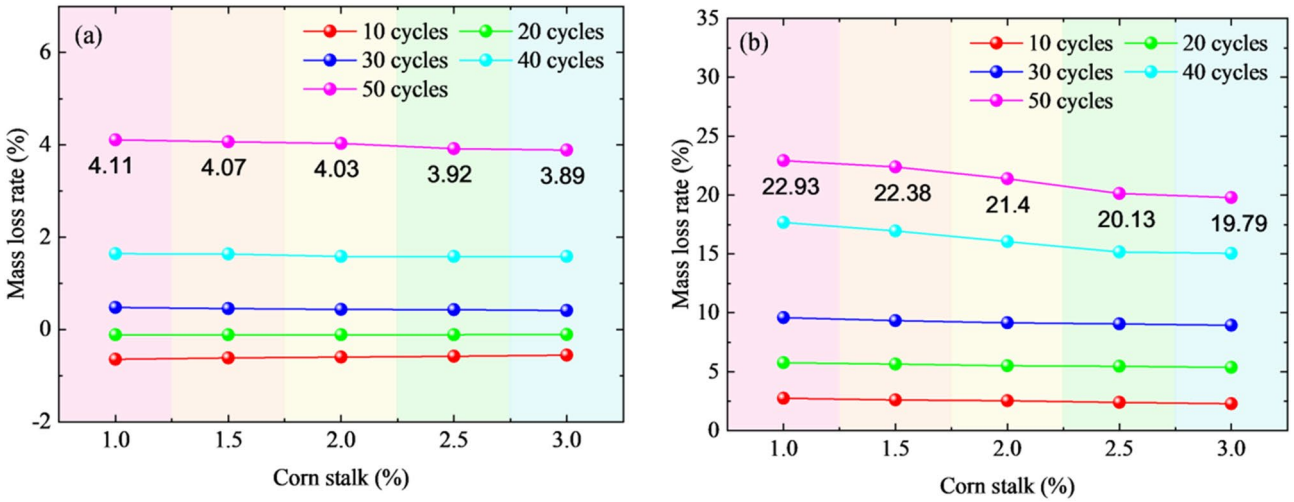

Fig. 13. (**a**) Mass loss and (**b**) compressive strength degradation of foamed concrete with varying corn stalk fiber content across multiple freeze-thaw cycles.

Conclusions

The study examined how foam content, SSP content, and CSF content influence SFSSFC performance. The following conclusions were found:

- The fluidity and water absorption of concrete are significantly affected by foam content. As foam content increases, porosity rises, thereby increasing the likelihood of water ingress, fluidity, and water absorption.
- Optimal mechanical strength is attained with a 15% SSP content. However, mechanical strength varies consistently with increasing foam and straw fiber content.
- Samples with similar dry density but lower thermal conductivity were prepared, exhibiting superior thermal insulation properties compared to materials in similar studies.
- After 30 freeze-thaw cycles, there was a notable increase in specimen mass loss and compressive strength. S15 exhibited excellent resistance to freezing and maintained its mechanical strength without any damage or destruction. Furthermore, straw fiber significantly improves the freeze-thaw performance of SFSSFC.

Data availability

No datasets were generated or analysed during the current study.

Received: 6 March 2025; Accepted: 19 June 2025
Published online: 01 July 2025

References

1. Chen, S., Zhang, G., Xia, X., Setunge, S. & Shi, L. A review of internal and external influencing factors on energy efficiency design of buildings. *Energy Build.* **216**, 109944. https://doi.org/10.1016/j.enbuild.2020.109944 (2020).
2. Feng, W. P., Jin, Y., Zheng, D., Li, Z. & Cui, H. Synergic effect of compositions and processing method on the performance of high strength alkali activated slag foam. *Constr. Build. Mater.* **352**, 128991. https://doi.org/10.1016/j.conbuildmat.2022.128991 (2022).
3. Huang, Y. et al. Experimental investigation on the influencing factors of Preparing porous fly ash-based geopolymer for insulation material. *Energy Build.* **168**, 9–18. https://doi.org/10.1016/j.enbuild.2018.02.043 (2018).
4. Shah, S. N., Mo, K. H., Yap, S. P., Yang, J. & Ling, T. Lightweight foamed concrete as a promising avenue for incorporating waste materials: A review, resources, conservation and recycling. **164**, 105103. https://doi.org/10.1016/j.resconrec.2020.105103 (2021).
5. Yi, H. et al. An overview of utilization of steel slag. *Procedia Environ.* **16**, 791–801. https://doi.org/10.1016/j.proenv.2012.10.108 (2012).
6. Li, H. B., Cui, C. Y., Cai, J. & Zhang, M. M. Utilization of steel slag in road semi-rigid base: a review. *Coatings* **12**, 2994. https://doi.org/10.3390/coatings12070994 (2022).
7. Chen, W. B., Wang, M. H., Liu, L. L., Wang, H. & Wang, X. D. Three-stage method energy-mass coupling high-efficiency utilization process of high-temperature molten steel slag. *Metall. Mater. Trans.* **52** (5), 3004–3015. https://doi.org/10.1007/s11663-021-02213-7 (2021).
8. Gan, Y. et al. Evaluation of the impact factors on the leaching risk of steel slag and its asphalt mixture, case stud. *Constr. Mater.* **16**, e01067. https://doi.org/10.1016/j.cscm.2022.e01067 (2022).
9. Domínguez, M. I. et al. Physicochemical characterization and use of wastes from stainless steel mill. *Environ. Prog Sustain. Energy*. **29** (4), 471–480. https://doi.org/10.1002/ep.10435 (2010).
10. Liao, Y., Jiang, G., Wang, K., Al Qunaynah, S. & Yuan, W. Effect of steel slag on the hydration and strength development of calcium sulfoaluminate cement. *Construct Build. Mater.* **265**, 120301. https://doi.org/10.1016/j.conbuildmat.2020.120301 (2020).
11. Rashad, A. M. Behavior of steel slag aggregate in mortar and concrete-A comprehensive overview. *J. Build. Eng.* **53**, 104536. https://doi.org/10.1016/j.jobe.2022.104536 (2022).
12. Xiang, G. et al. Investigation on Preparation and compressive strength model of steel slag foam concrete. *J. Building Eng.* **72**, 106548. https://doi.org/10.1016/j.jobe.2023.106548 (2023).
13. Li, M. et al. Enhancement in compressive strength of foamed concrete by ultra-fine slag. *Cem. Concr. Compos.* **138**, 104954. https://doi.org/10.1016/j.cemconcomp (2023).

14. Saini, K., Matsagar, V. A. & Kodur, V. R. Recent advances in the use of natural fibers in civil engineering structures. *Constr. Build. Mater.* **411**, 134364. https://doi.org/10.1016/j.conbuildmat.2023.134364 (2024).
15. Jin, Z., Mao, S., Zheng, Y. & Liang, K. Pre-treated corn straw fiber for fiber-reinforced concrete Preparation with high resistance to chloride ions corrosion. *Case Stud. Constr. Mater.* **19**, e02368. https://doi.org/10.1016/j.cscm.2023.e02368 (2023).
16. Rowell, R. The Use of Biomass To Produce bio-based Composites and Building Materials. Advances in Biorefineries, Woodhead Publishing, ed: Elsevier. 803–818. https://doi.org/10.1533/9780857097385.2.803 (2014).
17. Luo, Y. & Liu, H. Thermoelectric power generation in concrete: A study on influential material and structural factors. *Energy Build.* 115159–115159. https://doi.org/10.1016/j.enbuild.2024.115159 (2025).
18. Khan, A., Vijay, R., Singaravelu, D. L., Sanjay, M. & Siengchin, S. Extraction and characterization of natural fibers from Citrullus lanatus climber. *Nat. Fibers*. **19**, 621–629. https://doi.org/10.1080/15440478.2020.1758281 (2022).
19. Chen, C. et al. Comparative analysis of natural fiber reinforced polymer and carbon fiber reinforced polymer in strengthening of reinforced concrete beams. *J. Clean. Prod.* **263**, 121572. https://doi.org/10.1016/j.jclepro.2020.121572 (2020).
20. Malkapuram, R., Kumar, V. & Negi, Y. S. Recent development in natural fiber reinforced polypropylene composites. *Reinf Plast. Compos.* **28**, 1169–1189. https://doi.org/10.1177/0731684407087759 (2009).
21. Aquino, L. A. S., Silva, T. R. C., Marvila, M. T. & Azevedo, A. R. G. Agro-industrial waste from corn straw fiber: perspectives of application in mortars for coating and laying blocks based on ordinary Portland cement and hydrated lime. *Constr. Build. Mater.* **353**, 129111. https://doi.org/10.1016/j.conbuildmat.2022.129111 (2022).
22. Peng, D., Zhao, J., Liang, X., Guo, X. & Li, H. Corn stalk pith-based hydrophobic aerogel for efficient oil sorption. *J. Hazard. Mater.* **448**, 130954. https://doi.org/10.1016/j.jhazmat.2023.130954 (2023).
23. Ahmed, S. & Ali, M. Use of agriculture waste as short discrete fibers and glass-fiber-reinforced-polymer rebars in concrete walls for enhancing impact resistance. *J. Clean. Prod.* **268**, 122211. https://doi.org/10.1016/j.jclepro.2020.122211 (2020).
24. Tran, M. T., Vu, X. H. & Ferrier, E. Experimental and numerical investigation of carbon textile/cementitious matrix interface behaviour from pull-out tests. *Construct Build. Mater.* **282**, 122634. https://doi.org/10.1016/j.conbuildmat.2021.122634 (2021).
25. Hamada, H. M. et al. Application of natural fibres in cement concrete: A critical review. *Mater. Today Commun.* **35**, 105833. https://doi.org/10.1016/j.mtcomm.2023.105833 (2023).
26. Yooprasertchai, E., Wiwatrojanagul, P. & Pimanmas, A. A use of natural Sisal and jute fiber composites for seismic retrofitting of nonductile rectangular reinforced concrete columns. *J. Build. Eng.* **52**, 104521. https://doi.org/10.1016/j.jobe.2022.104521 (2022).
27. Balagopal, V., Panicker, A. S., Arathy, M. S., Sandeep, S. & Pillai, S. K. Influence of fibers on the mechanical properties of cementitious composites - a review. *Mater. Today Proc.* 651846–1850. https://doi.org/10.1016/j.matpr.2022.05.023 (2022).
28. Geremew, A., Outtier, A., De Winne, P., Demissie, T. A. & De Backer, H. An experimental investigation on the effect of incorporating natural fibers on the mechanical and durability properties of concrete by using treated hybrid Fiber-Reinforced concrete application. *Fibers* **13** https://doi.org/10.3390/fib13030026 (2025).
29. da Silva Neto, J. T. et al. Fiber-reinforced cementitious composites: recent advances and future perspectives on key properties for high-performance design. *Discover Civil Eng.* **2** https://doi.org/10.1007/s44290-025-00209-9 (2025).
30. Marzena, K., Magdalena, P. M., Yining, G. & Filip, K. The impact of natural fibers' characteristics on mechanical properties of the cement composites. *Sci. Rep.* **12** https://doi.org/10.1038/S41598-022-25085-6 (2022).
31. Lilargem Rocha, D. et al. A review of the use of natural fibers in cement composites: concepts, applications and Brazilian history. *Polymers* **14** https://doi.org/10.3390/polym14102043 (2022).
32. Rajkohila, A. & Prakash Chandar, S. Panruti thangaraj, r. Assessing the effect of natural fiber on mechanical properties and microstructural characteristics of high strength concrete. *Ain Shams Eng. J.* **15** https://doi.org/10.1016/j.asej.2024.102666 (2024).
33. Jarabo, R., Monte, M. C., Fuente, E., Santos, S. F. & Negro, C. Corn stalk from agricultural residue used as reinforcement fiber in fiber-cement production. *Industrial Crops Prod.* **43**, 832–839. https://doi.org/10.1016/j.indcrop.2012.08.034 (2013).
34. Saroj, D. et al. Characterization of natural Fiber extracted from corn (Zea mays L.) stalk waste for sustainable development. *Sustainability* **14**, 16605–16605. https://doi.org/10.3390/su142416605 (2022).
35. Bao, H. & Liu, Z. Manufacturing process of recycling corn fiber, A Low-tech materials for modular construction, phygital intelligence computational design and robotic fabrication Ch. *Chapter* **34**, 408–417. https://doi.org/10.1007/978-981-99-8405-3_34 (2024).
36. Chen, Z., Chen, Z., Yi, J. & Feng, D. Preparation method of corn stalk Fiber material and its performance investigation in asphalt concrete. *Sustainability* **11**, 4050–4050. https://doi.org/10.3390/su11154050 (2019).
37. Okeke, F. O., Ahmed, A., Imam, A. & Hassanin, H. A review of corncob-based Building materials as a sustainable solution for the Building and construction industry. *Hybrid. Adv.* **6**, 100269–100269. https://doi.org/10.1016/j.hybadv.2024.100269 (2024).
38. Dan, G., Maria, C. A., Marian, T. B., Catalin, P. A. & Raluca, N. Environmentally friendly cellulosic fibers from corn stalks. *Environ. Eng. Manag. J.* 171765–1771. https://doi.org/10.30638/eemj.2018.175. (2018).
39. Huang, Y. et al. Evaluating cement treated aggregate base containing steel slag: mechanical properties. *Volume Stab. Environ. Impacts Mater.* **15** (23), 8277–8277. https://doi.org/10.3390/ma15238277 (2022).
40. GB/T 2419 – 2005, *Test Method for Fluidity of Cement Mortar* (Standards Press of China, 2005).
41. Zhou, D., Gao, H., Liao, H., Fang, L. & Cheng, F. Enhancing the performance of foam concrete containing fly Ash and steel slag via a pressure foaming process. *J. Clean. Prod.* **329**, 129664. https://doi.org/10.1016/j.jclepro.2021.129664 (2021).
42. JG/T 266–2011, Foamed Concrete, Standards Press of China, Beijing, (2011).
43. Yao, T. et al. Laboratory investigation of foamed concrete prepared by recycled waste concrete powder and ground granulated blast furnace slag. *J. Clean. Prod.* **426**, 139095. https://doi.org/10.1016/j.jclepro.2023.139095 (2023).
44. 50081 – 2019, G. B. T. *Standard for Test Methods of Concrete Physical and Mechanical Properties* (China Construction Industry Press, Beijing, 2019).
45. JGJ/T341-2014. *Technical Specification for Application of Foamed Concrete* (China Construction Industry Press, Beijing, 2015).
46. 50082 – 2009, G. B. T. *Standard for Test Methods of long-term Performance and Durability of Ordinary Concrete* (China Construction Industry Press, Beijing, 2009).
47. Ren, J. et al. Experimental comparisons between one-part and normal (two-part) alkali-activated slag binders. *Constr. Build. Mater.* **309**, 125177. https://doi.org/10.1016/j.conbuildmat.2021.125177 (2021).
48. Osman Gencel, M. et al. Basalt fiber-reinforced foam concrete containing silica fume: an experimental study. *Constr. Build. Mater.* **326**, 126861. https://doi.org/10.1016/j.conbuildmat.2022.126861 (2022).
49. Bayraktar, O. Y. et al. Effect of cement dosage and waste tire rubber on the mechanical, transport and abrasion characteristics of foam concretes subjected to H_2SO_4 and freeze-thaw. *Constr. Build. Mater.* **302**, 124229. https://doi.org/10.1016/j.conbuildmat.2021.124229 (2021).
50. Gencel, O. et al. Characteristics of hemp fibre reinforced foam concretes with fly Ash and Taguchi optimization. *Constr. Build. Mater.* **294**, 123607. https://doi.org/10.1016/j.conbuildmat.2021.123607 (2021).
51. Nambiar, E. & Ramamurthy, K. Air-void characterisation of foam concrete. *Cem. Concrete Res.* **37** (2), 221–230. https://doi.org/10.1016/j.cemconres.2006.10.009 (2007).
52. Hilal, A. A., Thom, N. H. & Dawson, A. R. Pore structure and permeation characteristics of foamed concrete. *J. Adv. Concr. Technol.* **12** (12), 535–544. https://doi.org/10.3151/jact.12.535 (2014).
53. Li, L. G., Feng, J. J., Zhu, J., Chu, S. H. & Kwan, A. K. H. Pervious concrete: effects of porosity on permeability and strength. *Magazine Concrete Res.* **73** (2), 69–79. https://doi.org/10.1680/jmacr.19.00194 (2021).

54. Gencel, O., Oguz, M., Gholampour, A. & Ozbakkaloglu, T. Recycling waste concretes as fine aggregate and fly Ash as binder in production of thermal insulating foam concretes. *J. Building Eng.* **38**, 102232. https://doi.org/10.1016/j.jobe.2021.102232 (2021).
55. Zhang, S., Qi, X., Guo, S. & Ren, L. J. A systematic research on foamed concrete: the effects of foam content, fly ash, slag, silica fume and water-to-binder ratio. *Constr. Build. Mater.* **339**, 127683. https://doi.org/10.1016/j.conbuildmat.2022.127683 (2022).
56. Vinith Kumar, N., Arunkumar, C. & Srinivasa Senthil, S. Experimental study on mechanical and thermal behavior of foamed concrete. *Mater. Today: Proc.* **5** (2, Part 3), 8753–8760. https://doi.org/10.1016/j.matpr.2017.12.302 (2018).
57. Li, G. et al. The influence of wet ground fly Ash on the performance of foamed concrete. *Constr. Build. Mater.* **304**, 124676. https://doi.org/10.1016/j.conbuildmat.2021.124676 (2021).
58. Chen, X., Yan, Y., Liu, Y. & Hu, Z. Utilization of Circulating fluidized bed fly Ash for the Preparation of foam concrete. *Constr. Build. Mater.* **54**, 137–146. https://doi.org/10.1016/j.conbuildmat.2013.12.020 (2014).
59. Kearsley, E. P. & Wainwright, P. J. Porosity and permeability of foamed concrete. *Cem. Concr. Res.* **31** (5), 805–812. https://doi.org/10.1016/S0008-8846(01)00490-2 (2001).
60. Hao, Y., Yang, G. & Liang, K. Development of fly Ash and slag based high-strength alkali-activated foam concrete. *Cem. Concr. Compos.* **128**, 104447. https://doi.org/10.1016/j.cemconcomp.2022.104447 (2022).
61. Gopalakrishnan, R., Sountharajan, V. M., Mohan, A. & Tholkapiyan, M. The strength and durability of fly Ash and quarry dust light weight foam concrete. *Mater. Today: Proc.* **22**, 1117–1124. https://doi.org/10.1016/j.matpr.2019.11.317 (2020).
62. He, J., Gao, Q., Song, X., Bu, X. & He, J. Effect of foaming agent on physical and mechanical properties of alkali-activated slag foamed concrete. *Constr. Build. Mater.* **226**, 280–287. https://doi.org/10.1016/j.conbuildmat.2019.07.302 (2019).
63. Ahmadi, S. F., Reisi, M. & Amiri, M. C. Reusing granite waste in eco-friendly foamed concrete as aggregate. *J. Building Eng.* **46**, 103566. https://doi.org/10.1016/j.jobe.2021.103566 (2022).
64. Bayraktar, O. Y., Kaplan, G., Gencel, O., Benli, A. & Sutcu, M. Physico-mechanical, durability and thermal properties of basalt fiber reinforced foamed concrete containing waste marble powder and slag. *Constr. Build. Mater.* **288**, 123128. https://doi.org/10.1016/j.conbuildmat.2021.123128 (2021).
65. JGJ/T 341– Test methods for concrete durability, China Construction Industry Press, Beijing, 2014. (2014).

Acknowledgements

The financial support is provided by the Basic Scientific Research Business Cost Scientific Research Project of Heilongjiang Provincial Colleges and Universities, Young Innovative Talents Project (No. 145109208).

Author contributions

Yang Liu: Methodology, Software, Formal analysis, Investigation, Visualization, Writing - original draft. Shijie Fan: Writing - review & editing, Supervision. Qing Li: Conceptualization, Methodology, Formal analysis, Writing - original draft, Supervision.Hongbao Liang: Conceptualization, Methodology, Software, Formal analysis, Investigation, Visualization, Writing - original draft, Writing - review & editing. Xiaoyu Wang: Conceptualization, Methodology, Formal analysis, Writing - original draft, Supervision, Writing - review & editing. Jiaxi Xu: Investigation, Writing - original draft, Visualization.

Declarations

Competing interests

The authors declare no competing interests.

Additional information

Supplementary Information The online version contains supplementary material available at https://doi.org/10.1038/s41598-025-08149-1.

Correspondence and requests for materials should be addressed to H.L.

Reprints and permissions information is available at www.nature.com/reprints.

Publisher's note Springer Nature remains neutral with regard to jurisdictional claims in published maps and institutional affiliations.